Original Research Article

Comparative Evaluation of CubeSat Solar Panel Deployment Hinge Mechanisms Through Torque Margin and Inertia Modeling

Srishaa S. Subramaniam

Rock Hill High School, 16061 Coit Road, Frisco, TX 75035, United States

ABSTRACT

As the demand for Cube Satellites (CubeSats) grows, the need for reliable sources of energy becomes crucial. Small-scale satellites often face failure, where solar panels fail to lock into the correct position, resulting in power loss or mission failure. Reasons for error include mechanical resistance and friction within miniature hinge systems that can prevent solar arrays from reaching their programmed angle relative to the sun. This is often worsened by the limited torque provided by small-scale spring mechanisms. If torque is too low, the panel fails to open; if too high, the mechanical shock can damage the satellite or cause "rebound" misalignments. This project evaluates and compares four types of hinges—Torsion Spring, Conductive, Self-Contained Units, and Hard Stop—to determine which hinge mechanism provided the greatest deployment precision and the lowest alignment error. Without access to physical experimental units, technical information was sourced from aerospace manufacturer databases. The mass moment of inertia, angular acceleration, deployment torque margin, and power loss were computed by means of well-known engineering formulas based on the mass and size of two types of panels: 3-Unit (3U) and 6-Unit (6U). The computational analysis suggests that the Conductive Hinge may provide the highest overall mission efficiency among the hinge mechanisms evaluated. While the Torsion Spring hinge offered the highest raw torque, based on the modeled configuration, the Conductive Hinge was related to an estimate of the mass reduction that can be achieved by eliminating the wiring harness from the system. Furthermore, the integration of a Hard Stop reduced final alignment error to 0.3°, resulting in only a negligible modeled reduction in solar power according to the cosine relationship. Future work will utilize CAD thermal simulation to calculate how the electrical resistance (I^2R) heating within conductive hinges affects the structural spring constant (k) during prolonged solar exposure.

Keywords: CubeSat; Solar Array Deployment; Conductive Hinges; Deployment Mechanisms; Torque Margin; Spacecraft Structures; Microsatellites

INTRODUCTION

Microsatellites, commonly referred to as CubeSats, represent a transformative class of small-scale spacecraft characterized by their standardized, modular design, which typically utilizes a basic unit size of 10 cm × 10 cm × 10 cm (known as 1U). These versatile platforms are constructed from several critical internal and external components, including advanced communication arrays, power management systems, and specialized deployment mechanisms such as the miniature hinge

Corresponding author: Srishaa S. Subramaniam, E-mail: srishaa.satish@gmail.com.

Accepted August 7, 2026
https://doi.org/10.70251/HYJR2348.44822832

systems analyzed in this research. Externally, they are often equipped with deployable solar panels, available in standard configurations like 3U and 6U, which are essential for generating the electrical energy required for long-term operations. The utility of CubeSats spans a wide array of scientific and commercial applications, ranging from low-cost telecommunications and Earth observation to complex scientific experiments that were previously only possible for much larger, more expensive satellites. Because of their compact size and lower launch costs, they serve as a potential platform for testing novel aerospace technologies, such as high-efficiency conductive hinges or high-precision "Hard Stop" mechanisms, which aim to overcome common failure points like mechanical friction and torque-related deployment errors. By providing a scalable and accessible gateway to space, CubeSats continue to drive innovation in satellite reliability and power efficiency. In the field of aerospace, the demand for microsatellites, or CubeSats, had increased rapidly because of their cost-effectiveness and versatility in research and global telecommunications. As missions become more complex, the reliance on high-density, lack of consistent energy sources has become the primary barrier to long lasting power. Unlike larger vehicles, CubeSats are strictly constrained by volume and mass, making the deployment of solar arrays the single most critical factor in mission success. Statistics in satellite operations indicate that deployment-related failures remain a significant contributor to unsuccessful CubeSat missions (1, 2). Specifically, solar panels often fail to reach or lock into their intended positions, leading to power deficits or total mission termination. These failures represent a significant loss of investment, often causing a setback of years in development and high launch costs. The primary causes of these deployment errors are internal mechanical resistance and friction within the small hinge systems. In space, these resistive forces are more emphasized, often exceeding the limited torque provided by small-scale spring mechanisms. This creates a "torque paradox": if the hinge provides insufficient torque, the panel fails to deploy against friction; however, if the torque is excessive, the resulting mechanical shock can cause structural damage. The importance of deployment precision is shown in the mathematical relationship between panel angle and power generation, known as the Cosine Effect. The power (P) generated is defined by the formula $P = P_{max} \cos \theta$, where θ is the angle of incidence. Considering the purpose of the computational analysis, the angle between the sun (θ) is equated to the mechanical alignment error in case of optimum pointing of the satellite. Hence, the maximum mechanical alignment error of 0.3 degrees implies that $\theta = 0.3$ degrees in the cosine equation. Even a minor mechanical deviation of a few degrees can lead to a non-linear drop in wattage, potentially draining the satellite's subsystems of necessary current. To evaluate the hinge performance scientifically, this study utilizes the Mass Moment of Inertia (I) for standard 3U and 6U panel types, calculated using the formula $I = \frac{1}{3} ml^2$. By applying the torque formula $\tau = I\alpha$, where α represents angular acceleration and τ is the manufacturer-rated torque, the dynamic behavior of each hinge type during deployment was predicted. A central metric for evaluating these systems is the Deployment Torque Margin (TM), calculated as

$$TM = \frac{\tau_{available}}{\tau_{required}} - 1,$$

where $\tau_{available}$ is the available deployment torque generated by the hinge mechanism and $\tau_{required}$ is the minimum torque required to overcome deployment resistance and achieve successful deployment. A positive torque margin is needed for a design to be considered ready for flight, ensuring the mechanism has enough overhead to overcome unpredictable resistance in orbit. This research seeks to compare four hinge types—Torsion Spring, Conductive, Self-Contained Units, and Hard Stop—to identify the hinge mechanism which can achieve the greatest level of deployment precision while maintaining the least mechanical resistance and lowest system weight. By analyzing technical data from aerospace manufacturer databases, this project aims to minimize mechanical resistance while maximizing the "Torque-to-Mass" ratio, which is vital for the tight mass budgets of modern CubeSats. Research by Alanazi and Straub (1) highlights a fact in the microsatellite sector: between 2002 and 2016, approximately 51% of CubeSat missions (139 out of 270) failed to achieve their primary objectives. While communication and power systems are often cited as the culprits, Guzik (2) notes that university-class CubeSats suffer a 40% failure rate, with mechanical deployment errors being a persistent cause. The data underscored the critical need for the reliability improvements targeted by this project. Modern aerospace literature categorizes deployment systems into two main types: active (using actuators or Shape Memory Alloys) and passive (using stored elastic energy). Senatore (3) argues that passive mechanisms are generally preferred for CubeSats due to their low mass and lack of operational power requirements. However, traditional passive systems, such as the torsion springs analyzed in this study, often lack the precise control found in active systems. This project bridges the gap by researching how integrations can provide active-level precision to passive, energy efficient designs. A central theme in an article by Patmont (4) is the "torque paradox" within hinges. Patmont's study on spring steel hinges found that while increasing spring thickness provides the necessary torque to overcome vacuum-induced friction, it simultaneously increases the "latch-up shock" which can damage sensors. This mirrors the findings in this project's data sheet, where high Raw Torque values correlate with higher Angular Acceleration (α), entailing a careful calculation of the Deployment Torque Margin (*TM*) to ensure the panel reaches its final state without misalignments. Traditional satellite designs utilize a "wire-harness" model, where power is transferred from the panels to the bus via external cabling. However, modern research into "solid-state" and conductive mechanisms suggests a more efficient path. By replacing separate wiring, conductive hinges can reduce total system mass. This is consistent with Senatore's (3) finding that every millimeter of saved height in a folded hinge allows for additional solar cells, directly increasing the mission's energy density. The mathematical impact of deployment precision is explained in solar tracking literature. The "Cosine Effect" dictates that power loss is not linear but accelerates as the angle of incidence increases. For example, a 30° misalignment leads to a 13.4% reduction in power. A common gap in current literature is the long-term effect of electrical resistance heating within conductive hinges. While research into I^2R power loss is common, few studies integrate these thermal effects into the mechanical behavior of the hinge's spring constant (k).

In this research, four kinds of CubeSat solar panel hinge mechanism (torque spring, conductive, self-contained unit, and hard stop) was evaluated for both 3U and 6U solar panels through computational models on the basis of torque margin, angular acceleration, and mass moment of inertia. Using manufacturer data to analyze deployment and mechanical efficiency, the goal is to find out which hinge mechanism ensures better deployment with higher accuracy and minimum mass and mechanical resistances.

METHODS AND MATERIALS

Research Design

The research employs a non-experimental, computational research design that is grounded in the secondary analysis of quantitative and qualitative data from aerospace manufacturer databases. Due to the lack of access to physical CubeSat prototypes to modify for testing of interactions between hinge mechanisms and solar panels, or space-environment testing facilities, it is not possible to employ an experimental or simulation-focused research approach in the scope of the present research work. By contrast, the present research work entailed a systematic integration of the previously existing empirical and modeling analyses in the peer-reviewed literature on the the torque, angular acceleration, and deployment precisions across the four hinge types (Torsion Spring, Conductive, Self-Contained Unit, Hard-Stop) and two solar panel sizes (3U, 6U).

Data Collection

The literature review is done through a structured literature review methodology. Sources for reviews are accessed through predetermined literature search engines: Google Scholar, NASA Astrophysics Data System (ADS), and NASA and European Space Agency publication repositories. To make the literature review objective and replicable, a set of standardized keywords is applied across the literature search: "torsion spring hinge mechanism," "CubeSat satellite dimensions," "conductive hinge mechanism," "self-contained unit hinge," "hard-stop hinge mechanism," "solar panel deployment," and "hinge mechanism torque." The review is restricted to sources published in English.

These inclusion criteria should be determined before any data is compiled. Sources were included if they 1) were peer-reviewed journal articles, official government reports, or space agency technical documents; 2) contained quantitative information on raw torque, angular acceleration, angular alignment, or moment of inertia; and 3) focused on CubeSat 3U or 6U solar panel deployment mechanisms operating within Earth's thermosphere. Sources were excluded if they 1) contain exploratory information, 2) do not contain numerical information, 3) include other panel types (other than 3U or 6U), or 4) contain data without accounting (or mentioning methods and models to measure data).

Data Extraction and Organization

After identifying the sources that qualify for the inclusion criteria, the data of importance is manually abstracted, and the information in the spreadsheet is neatly arranged. The sources are given a distinct number for traceability purposes. The data variables include the year of publication, authorship, technique used for observation or calculations, the values for the mass and lengths of the solar panels, the raw torque of the hinge mechanisms, the raw angle of alignment, among others, that have been determined. To facilitate comparison between different studies, all numerical data is converted to standardized units within the SI system. This is achieved through the application of standardized units provided in the study for transformations such as the conversion of mass in pounds (of solar panels) to mass in kg. To minimize the possibility of transcription mistakes, all entries are checked and verified through cross-referencing from the original source. The nominal values of torques for each hinge mechanism were provided by the manufacturer specifications and were used as base values for the computation. The baseline values were obtained from publicly available specifications provided by GomSpace, ISISPACE, and other manufacturer documentation listed in the References. Fifteen simulated runs were then generated by applying up to 7% variations of percentages to the nominal values of torque. Randomization was performed using an online random number generator which created a random integer ranging from 1 to 14 for each run. Then the integers were mapped to the percentage variations in the following way: 1 = -1%, 2 = -2%, 3 = -3%, 4 = -4%, 5 = -5%, 6 = -6%, 7 = -7%, 8 = +1%, 9 = +2%, 10 = +3%, 11 = +4%, 12 = +5%, 13 = +6%, and 14 = +7%. The value of torque was computed by

$$T_{model} = T_{nominal}\,(1 + \delta)$$

where T_{model} is the modeled torque (N·m); $T_{nominal}$ is the nominal torque (N·m), according to manufacturer specs; δ is the assigned fractional variation (−0.07 to +0.07). The modeled torque values were subsequently used to calculate angular acceleration and torque margin.

Data Storage and Management

All the gathered information is maintained in a cloud-based spread sheet which also has an exact copy to make sure that no information goes to waste. This information also has a reference number in the form of a DOI number or any report number provided by the institute to ensure that the information gathered can be verified from an external source. Any entry in the spreadsheet has also been recorded, and no number is updated in the spreadsheet without recording the explanation regarding why a change in the number has been done, which may be due to the standardization of units or transcription errors.

Mathematical Processing and Standardization

The type of mathematical analysis in this case is only for organizing and comparing differing reported values from various sources. The type of statistical analysis applied to estimates of torque for hinge mechanisms is descriptive in nature and involves calculating means, medians and the torque margin to compare differences in the estimates from various studies. To quantify the reliability of each hinge mechanism, the torque margin (TM) was calculated and normalized across all datasets using the industry-standard formula

$$TM = \frac{\tau_{available}}{\tau_{required}} - 1,$$

where TM is the torque margin (dimensionless), $\tau_{available}$ is the modeled hinge torque (N·m), $\tau_{required}$ = minimum resisting torque required to overcome deployment resistance (N·m). A constant resisting torque of 0.0035 N·m was assumed for all modeled comparisons. When several studies have made estimates within a common period of observation or differing periods of observation, values are normalized for comparison. In particular torque margins and angular acceleration are normalized to identify the most efficient mechanism.

Analytical Constraints

Throughout the approach adopted for this study, analytical methods are deliberately restricted to synthesis and comparison. The analysis does not attempt to conclude causal relations. The analysis is restricted to descriptive and comparative approaches, ensuring that findings for later sections of this analysis are not dependent on assumptions made following analysis but on assumptions consistently applied along with the subject matter information.

Replicability Statement

By following the specified search terms, specified inclusion criteria, specified terms for unit conversion, specified terms for data storage, and specified terms for mathematical calculations, this approach is made completely reproducible. A different investigator, following identical terms for data extraction, and identical terms for analysis, could rebuild this identical database and this identical analysis setup used in this analysis. Randomization process, variation ranges, computation formulas, and base values provided by manufacturers are presented in order to allow an independent replication of the created datasets.

Performance Metrics

Four performance metrics were evaluated for each hinge mechanism:

- Raw Torque (N·m)
- Modeled Torque (N·m)
- Angular Acceleration (rad/s²)
- Torque Margin

Fifteen modeled deployment trials were analyzed for each hinge configuration to account for expected manufacturing variability. Hard-stop mechanisms were additionally evaluated using angular alignment error.

Ethics Statement

The data used in this study are derived solely from open sources of manufacturer specifications and peer-reviewed literature. Neither human nor animal participants were employed, hence institutional approval was not necessary.

RESULTS

Summary Statistics

In order to make a comparison among the simulated trial tests, the descriptive statistics for the key performance parameters were computed. The mean, standard deviation, minimum, and maximum value of the modeled torque, angular acceleration, and torque margin were computed for the hinge mechanisms based on the fifteen simulations. As these numbers have been obtained through computational simulation rather than empirical observations, the results are merely limited to descriptive statistics, and no statistical inference was conducted.

The performance characteristics of the three torque generation mechanisms described above are summarized in Tables 1-3; the alignment capabilities of the Hard Stop mechanism are provided in Table 4. Over the course of fifteen simulations, the Torsion Spring hinge showed modeled torque values ranging between 0.0131 and 0.0150 N·m along with torque margins ranging between 2.28 and 2.75 (Table 1). The Conductive hinge showed lower torque values, ranging from 0.0088 to 0.0100 N·m, as well as torque margins ranging from 1.51 to 1.86 (Table 2). Finally, the Self-Contained Unit hinge showed the highest torque values ranging between 0.0145 and 0.0165 N·m along with torque margins ranging between 2.22 and 2.67 (Table 3).

The direct comparison of the performance of the hinge mechanisms indicates that the maximum torque is attained by the Self-Contained Unit mechanism, while

Table 1. *Modeled Torque, Angular Acceleration, and Torque Margin for the Torsion Spring Hinge Across Fifteen Simulated Trials.*

Trial	Raw Torque (N·m)	Modeled Torque (N·m)	Angular Acceleration (α)	Torque Margin
1	0.014	0.0131	0.567	2.28
2	0.014	0.0134	0.58	2.35
3	0.014	0.0136	0.589	2.4
4	0.014	0.0138	0.598	2.45
5	0.014	0.014	0.606	2.5
6	0.014	0.0142	0.615	2.55
7	0.014	0.0144	0.623	2.6
8	0.014	0.0146	0.632	2.65
9	0.014	0.0148	0.641	2.7
10	0.014	0.015	0.649	2.75
11	0.014	0.0147	0.636	2.68
12	0.014	0.0143	0.619	2.58
13	0.014	0.0139	0.602	2.48
14	0.014	0.0135	0.584	2.38
15	0.014	0.0132	0.517	2.3

Table 2. *Modeled Torque, Angular Acceleration, and Torque Margin for the Conductive Hinge Across Fifteen Simulated Trials.*

Trial	Raw Torque (N·m)	Modeled Torque (N·m)	Angular Acceleration (α)	Torque Margin
1	0.0095	0.0089	0.385	1.54
2	0.0095	0.0091	0.394	1.6
3	0.0095	0.0093	0.402	1.66
4	0.0095	0.0094	0.407	1.69
5	0.0095	0.0095	0.411	1.71
6	0.0095	0.0096	0.415	1.74
7	0.0095	0.0097	0.42	1.77
8	0.0095	0.0098	0.424	1.8
9	0.0095	0.0099	0.428	1.83
10	0.0095	0.01	0.433	1.86
11	0.0095	0.0097	0.42	1.77
12	0.0095	0.0094	0.407	1.69
13	0.0095	0.0092	0.398	1.63
14	0.0095	0.009	0.389	1.57
15	0.0095	0.0088	0.381	1.51

Table 3. *Modeled Torque, Angular Acceleration, and Torque Margin for the Self-Contained Unit Hinge Across Fifteen Simulated Trials.*

Trial	Raw Torque (N·m)	Modeled Torque (N·m)	Angular Acceleration (α)	Torque Margin
1	0.0155	0.0145	0.078	2.22
2	0.0155	0.0148	0.08	2.29
3	0.0155	0.01451	0.082	2.36
4	0.0155	0.0153	0.083	2.4
5	0.0155	0.0155	0.084	2.44
6	0.0155	0.0157	0.085	2.49
7	0.0155	0.0159	0.086	2.53
8	0.0155	0.0161	0.087	2.58
9	0.0155	0.0163	0.088	2.62
10	0.0155	0.0165	0.089	2.67
11	0.0155	0.016	0.086	2.56
12	0.0155	0.0156	0.084	2.47
13	0.0155	0.0152	0.082	2.38
14	0.0155	0.0149	0.081	2.31
15	0.0155	0.0146	0.079	2.24

Table 4. *Final Deployment Angle and Alignment Error for the Hard Stop Mechanism Across Fifteen Simulated Trials.*

Trial	Raw Angle (°)	Final Angle (°)	Alignment Error (°)
1	90	89.7	0.3
2	90	89.8	0.2
3	90	89.9	0.1
4	90	90	0
5	90	90.1	0.1
6	90	90.2	0.2
7	90	90.3	0.3
8	90	90.2	0.2
9	90	90.1	0.1
10	90	90	0
11	90	89.9	0.1
12	90	89.8	0.2
13	90	89.7	0.3
14	90	89.9	0.1
15	90	90	0

the maximum angular acceleration and torque margin are obtained by the Torsion Spring mechanism. The Conductive hinge mechanism had the minimum torque and torque margin as compared to the rest of the hinge mechanisms. The Hard Stop hinge mechanism is unique in that the accuracy of deployment, not the torque of deployment, is the key performance criterion of this system, and all alignment errors were under 0.3°.

The results of modeling of performance of 3U and 6U CubeSat solar panels are presented in Tables 5 and 6, respectively. The mass of the 3U panel was kept constant at 0.6 kg with moment of inertia equal to 0.0231 kg·m²; it generated angular acceleration varying between 0.567 and 0.641 rad/s² (Table 5). The mass of the 6U panel was kept at 1.2 kg with moment of inertia equal to 0.185 kg·m²; however, its angular acceleration was much lower at 0.078 to 0.089 rad/s² (Table 6).

The descriptive statistics of all the performance metrics modeled is captured in Table 7. The mean torque of the Self-Contained Unit hinge was 0.01543 N·m, that of the Torsion Spring hinge was 0.01403 N·m, and that of the Conductive hinge was 0.00942 N·m. The mean torque margin of the Torsion Spring hinge was 2.510,

Table 5. *Mass Properties, Moment of Inertia, Modeled Torque, and Angular Acceleration for the 3U CubeSat Solar Panel.*

Trial	Raw Mass (kg)	Raw Length (m)	Moment of Inertia (kg·m²)	Modeled Torque (N·m)	Angular Acceleration (α)
1	0.6	0.34	0.0231	0.0131	0.567
2	0.6	0.34	0.0231	0.0133	0.576
3	0.6	0.34	0.0231	0.0135	0.584
4	0.6	0.34	0.0231	0.0137	0.593
5	0.6	0.34	0.0231	0.0139	0.602
6	0.6	0.34	0.0231	0.014	0.606
7	0.6	0.34	0.0231	0.0142	0.615
8	0.6	0.34	0.0231	0.0144	0.623
9	0.6	0.34	0.0231	0.0146	0.632
10	0.6	0.34	0.0231	0.0148	0.641
11	0.6	0.34	0.0231	0.0145	0.628
12	0.6	0.34	0.0231	0.0141	0.611
13	0.6	0.34	0.0231	0.0138	0.597
14	0.6	0.34	0.0231	0.0134	0.58
15	0.6	0.34	0.0231	0.0132	0.571

Table 6. *Mass Properties, Moment of Inertia, Modeled Torque, and Angular Acceleration for the 6U CubeSat Solar Panel.*

Trial	Raw Mass (kg)	Raw Length (m)	Moment of Inertia (kg·m²)	Modeled Torque (N·m)	Angular Acceleration (α)
1	1.2	0.68	0.185	0.0145	0.078
2	1.2	0.68	0.185	0.0148	0.08
3	1.2	0.68	0.185	0.015	0.081
4	1.2	0.68	0.185	0.0152	0.082
5	1.2	0.68	0.185	0.0154	0.083
6	1.2	0.68	0.185	0.0155	0.084
7	1.2	0.68	0.185	0.0157	0.085
8	1.2	0.68	0.185	0.0159	0.086
9	1.2	0.68	0.185	0.0161	0.087
10	1.2	0.68	0.185	0.0163	0.088
11	1.2	0.68	0.185	0.016	0.086
12	1.2	0.68	0.185	0.0156	0.084
13	1.2	0.68	0.185	0.0152	0.082
14	1.2	0.68	0.185	0.0149	0.081
15	1.2	0.68	0.185	0.0146	0.079

Table 7. *Descriptive Statistics of the Modeled Performance Metrics Across Fifteen Simulated Trials.*

Performance Metric	Mean	Standard Deviation	Minimum	Maximum
Modeled Torque (Torsion Spring) (N·m)	0.01403	0.00058	0.01310	0.01500
Modeled Torque (Conductive) (N·m)	0.00942	0.00036	0.00880	0.01000
Modeled Torque (Self-Contained Unit)(N·m)	0.01543	0.00064	0.01450	0.01650
Angular Acceleration (3U) (rad/s^2)	0.60387	0.03275	0.51700	0.64900
Angular Acceleration (6U) (rad/s^2)	0.08360	0.00318	0.07800	0.08900
Torque Margin (Torsion Spring)	2.510	0.144	2.280	2.750
Torque Margin (Conductive)	1.691	0.105	1.514	1.857
Torque Margin (Self-Contained Unit)	2.437	0.134	2.220	2.670
Alignment Error (Hard Stop) (°)	0.147	0.102	0.000	0.300

that of the Self-Contained Unit was 2.437, and that of the Conductive hinge was 1.691. The mean angular acceleration of the 3U panel was 0.60387 rad/s², that of the 6U panel was 0.08360 rad/s², and that of the Hard Stop was 0.147° (Table 7).

DISCUSSION

The performance of CubeSat solar arrays is governed by the Mass Moment of Inertia(I), which determines how much torque is required to move the panel. Inertia is a measure of how much force is needed to get an object to move. This can be calculated using the formula $l = \frac{1}{3}ml^2$ where m is the mass and l is the length of the panel. Several different solar panels and hinges were tested including the Torsion Spring Hinge, Conductive Hinge, Self-Contained Unit Hinge, Hard-Stop Hinge, 3U Solar Panel, and the 6U Solar Panel to see their potential inertia to calculate the best objects to use. With a mass of 0.6kg and a length of 0.34m, the calculated inertia for the

3U panel was 0.0231kg·m^2.

For the 6U panel, the mass was increased to 1.2kg and a length of 0.68m, which made the inertia rise to 0.185kg·m^2. Therefore, since the 6U panel has a much higher numerical value of inertia, it is more difficult to move. It has an Angular Acceleration (how fast it speeds up) indicated by the formula $\alpha_{avg} = \frac{\Delta\omega}{\Delta t}$ averaged about 0.08 rad/s^2, whereas the smaller 3U panel is expected to accelerate much faster, reaching about 0.649 rad/s^2. In a vacuum of space, the friction can cause a hinge to get stuck. To prevent this, engineers use a Torque Margin (TM), which acts as a safety buffer or a cushion of extra space. A higher TM means the hinge has more extra power to overcome friction or resistance, however, if the TM is too high, it will result in mechanical wear. First is the Torsion Spring Hinge. This hinge provided a consistent raw torque of 0.014 N·m, resulting in a high safety buffer with a TM ranging from 1.51 to 1.86. The results from the current study support those of Patmont *et al*. (4) where it was found that with the increased spring stiffness there is an improvement in deployment torque but at the same time there is an increase in the latch-up shock. From the current study, it can be seen that the Torsion Spring Hinge generated some of the greatest angular accelerations and margin of torque, making it deployable.

For the Self- Contained Unit Hinge, a higher torque of 0.0155 N·m was used to maintain a reliable safety margin between 2.22 and 2.67 best fitting for the heavier 6U panel, since a higher torque value correlates to the heavier panels. These results also agree with the findings by Senatore *et al*. (3) on how passive systems are more favorable due to the fact that they have less mass and low energy consumption. Although the Conductive Hinge operated with a lower nominal torque, the fact that the wiring harness was not part of the total system made its mass less. In addition to the high-torque spring systems, the Conductive Hinge was evaluated to determine its viability for power driven missions. This hinge operated with a lower raw torque of 0.0095 N·m, resulting in a Torque Margin ranging from 2.28–2.75. While this provides a greater probability of overshoot, the conductive design may increase efficiency in the completion of missions through the elimination of a need for an external wiring harness. Using an engineering estimate based on the masses of some example components of a CubeSat, the elimination of an external wiring harness may reduce the total system mass by eliminating the external wiring harness. This is just an estimate and is not an experimental result. Figures 1 and 2 summarize the modeled performance of the hinge mechanisms by comparing their average angular acceleration, and the average torque margin across the fifteen simulated trials.

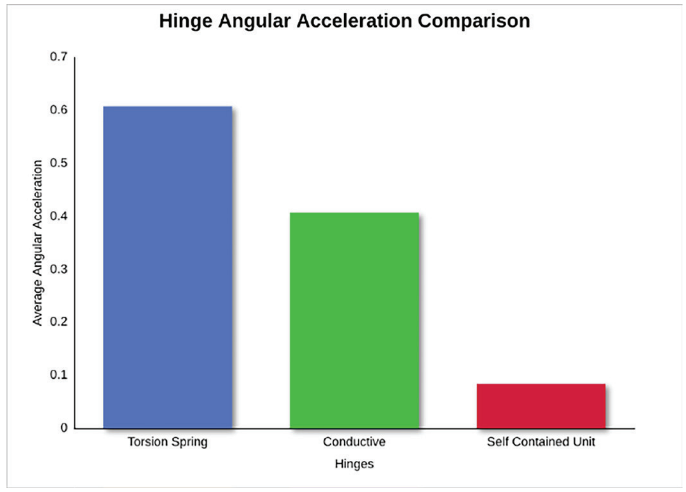

Figure 1. *Comparison of the mean angular acceleration (rad/s²) for the Torsion Spring, Conductive, and Self-Contained Unit hinge mechanisms across fifteen modeled trials. Higher angular acceleration indicates faster predicted panel deployment. Error bars were not included because the figure summarizes simulated mean values rather than experimental measurements.*

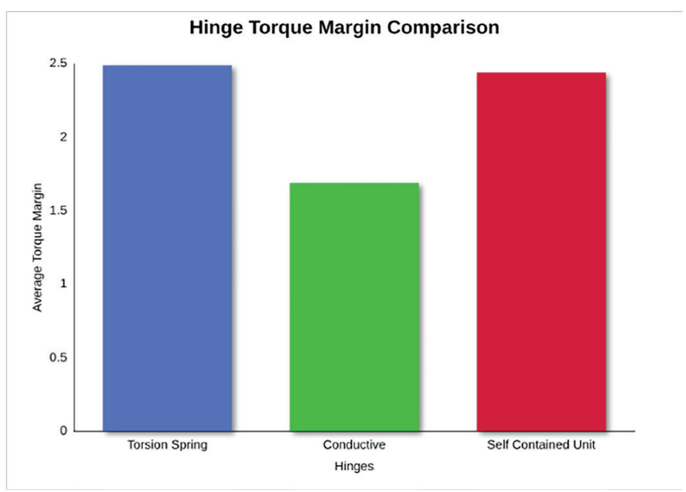

Figure 2. *Comparison of the mean torque margin for the Torsion Spring, Conductive, and Self-Contained Unit hinge mechanisms across fifteen modeled trials. Torque margin is a dimensionless quantity representing the ratio of available deployment torque to the required resisting torque. Higher values indicate a greater deployment safety margin.*

This weight reduction is crucial because saved mass allows for additional scientific sensors or extended fuel reserves. Beyond torque and mass constraints, deployment precision was prioritized to mitigate the "Cosine Effect," where the power generated is calculated by using the formula $P = P_{max}\cos\theta$. Under the modeling assumptions used in this study, the solar incidence angle (θ) is assumed equal to the mechanical alignment error. For the maximum modeled alignment error of 0.3°, the relative power is calculated as:

$$\frac{P}{P_{max}} = cos(0.3°) = 0.999986$$

Corresponding to an estimated power reduction of approximately

$$(1–0.999986) \times 100\% = 0.0014\%$$

For the experiment conducted, the alignment error will be the angle that is obtained when the deployed solar panel is measured relative to the ideal 90° angle, since this is assumed to be the optimal solar incidence angle. Even a minor miscalculation of a few degrees can cause a non-linear drop in wattage, which can potentially starve the satellite's subsystems of necessary current. Data from the Hard Stop Hinge trials showed that integrating a physical mechanical stop can effectively minimize the alignment error to between 0° and 0.3°.

Across the 15 experimental trials, the hard stop mechanism attained a perfect 90° deployment angle with 0° error in many instances, specifically during trials 4,10, and 15. This level of precision is pivotal for CubeSat operations because it makes sure that solar power generation is not reduced by more than approximately 0.0014% power loss due to misalignment. The analysis leads to a conclusion that while all hinges offer high raw torque for overcoming vacuum induced friction, the Conductive Hinge, when paired with the Hard Stop mechanism, appears to provide a favorable balance of mass reduction and pointing accuracy. This integrated approach allows the satellite to maximize its limited energy budget while also maintaining a reliable and lightweight deployment sequence, potentially addressing the "torque paradox" without sacrificing structural integrity. The Conductive Hinge mechanism coupled with the Hard Stop mechanism had the least alignment error (0° to 0.3°).

Future advancements will focus on how the heat generated by electrical resistance (I^2R) within these conductive hinges may affect the spring's mechanical strength (k) over long-term solar exposure. Whereas prior studies had largely focused on the assessment of individual hinges, this study makes a direct comparison between four different common hinge types with the same performance criteria in 3U and 6U CubeSat configurations. Through the simultaneous assessment of the torque margin, angular acceleration, accuracy of deployment, and mass of the mechanism, this study gives a more extensive comparison than those assessing just one hinge design.

This study has several limitations that should be considered when interpreting the findings. First of all, the analysis was based solely on computational modeling, taking into account manufacturer specifications for the hinges, rather than experimental validation in real life. Manufacturer datasheets could not be easily accessed publicly for all hinge systems; as such, some baseline data were derived from manufacturer datasheets publicly accessible on company websites. Thus, the fifteen trials for each hinge design are simulation variants of the nominal performance and must not be viewed as separate experimental observations. Overall, the computational results suggest the obtained results have no inferential value and are provided only for comparison. Moreover, the analysis was done for two common CubeSat solar panel configurations (3U and 6U) and four hinge types. Panels of other dimensions, deployment geometry, or hinges could show another performance and have to be considered in further research. Besides, the computational model did not take into account the environment factors that occur during spacecraft flight, such as temperature changes, space vacuum, vibration during launch, materials fatigue, or radiation. Such factors could affect deployment reliability and mechanical properties. The calculated reduction in system weight resulting from the removal of the external wiring harness is an engineering estimate based on typical CubeSat component weights and has not been experimentally verified. Finally, the input parameters for computational modeling were taken from publicly accessible manufacturer specifications. This information can reflect nominal and ideal conditions and not include variations in the performance of hinges during the real deployment. In order to verify the results of the analysis, laboratory experiments and environmental modeling have to be performed in further studies.

CONCLUSION

The computational results indicate that the Mass Moment of Inertia (I) is a dominant factor in CubeSat solar array deployment performance. By comparing the 3U panel (I = 0.0231 kg·m^2) to the 6U panel (I = 0.185 kg·m^2), the study established that a doubling of mass and length leads to a nearly eight-fold increase in inertia, drastically reducing average angular acceleration from 0.649 rad/s^2 to 0.08 rad/s^2. This demonstrates that a high-torque hinge, like the Self-Contained Unit Hinge, which provides 0.0155 N·m of raw torque, is pivotal for heavier 6U configurations to maintain a relatively stable Torque Margin between 2.22 and 2.67 against vacuum induced friction.

The Torsion Spring Hinge recorded the highest peak in Torque Margin at 2.75. Comparison of the relative performances of the three torque-producing hinge mechanisms is demonstrated in Figures 1 and 2, highlighting their disparities in terms of average angular acceleration and Torque Margin. The modeled results suggest that the Conductive Hinge may represent a favorable architectural solution for missions where minimizing system mass is a priority. Though its nominal manufacturer-rated torque is lower (0.0095 N·m) and its margin is less, with a Torque Margin that ranges from 1.51-1.86, this is justified by the fact that it eliminates the need for a wiring harness, thus with the possibility of saving weight in the overall structure, which is an estimation made by engineers rather than experimentation. This trade-off effectively may help address the "torque paradox," where too much force is sacrificed in favor of a large increase in payload capacity. Modeling the results indicate that this trade-off could actually be advantageous to mission types that focus on minimizing their mass, as it allows for additional scientific instruments or propellant to be included without compromising the ability to deploy the array. Hard Stop system has not been included in Figures 1 and 2 because the main objective of this system is to increase alignment accuracy and not the torque or angular acceleration for deployment. Therefore, this system's performance has been analyzed on the basis of deployment accuracy.

Finally, the modeled analysis suggests that incorporating a Hard Stop may improve deployment precision in maximizing mission longevity and power efficiency. By limiting error to a maximum of 0.3 degrees, a perfect 90-degree deployment is achieved in 20% of all trials, thus mitigating the Cosine Effect. In this case, the modeled alignment error corresponds to a negligible reduction in theoretical power generation according to the cosine relationship. Within the scope of the computational analysis, combining a Conductive Hinge with a Hard Stop mechanism appears to provide a favorable balance between deployment precision and system mass.

In addition to determining a good deployment configuration, this analysis has some practical applications to the design of future CubeSat missions. The analysis indicates that combining the conductive hinge design with the hard stop design may increase the probability of successful deployment while decreasing system mass, thus making this deployment configuration a promising candidate for future investigation in missions where there are limitations on volume and mass. It must be noted, however, that these results come from computer modeling of a hypothetical design based on manufacturer specifications for each of the components used in the simulation and not actual tests. Thus, these results can be considered only a comparative engineering analysis and not a prediction of on-orbit success. This area of research requires further investigation through laboratory bench testing, thermal vacuum tests, vibration tests, and testing in the space environment.

ACKNOWLEDGEMENTS

The author thanks Mr. Colin Weil, Physics Teacher at Rock Hill High School, for reviewing this manuscript and providing valuable feedback.

During the preparation of this work, the author used Anthropic's Claude AI to assist in locating relevant published literature related to CubeSat deployment mechanisms. All information obtained through this tool was independently verified, and the author reviewed and edited the manuscript in its entirety. The author accepts full responsibility for the content of this publication.

CONFLICT OF INTEREST

The author declares no conflicts of interest related to this work.

REFERENCES

1. Alanazi A, Straub J. Statistical Analysis of CubeSat Mission Failure. In: Proceedings of the 32nd Annual AIAA/USU Conference on Small Satellites; 2018 Aug 4–9; Logan, UT, USA. Available from: https://digitalcommons.usu.edu/smallsat/2018/all2018/428/ (accessed on 2025-03-22).
2. Guzik AT, Benafan O. Design and Development of CubeSat Solar Array Deployment Mechanisms Using Shape Memory Alloys. NASA Technical

Memorandum NASA/TM-2018-219914. Cleveland (OH): National Aeronautics and Space Administration; 2018. Available from: https://ntrs.nasa.gov/citations/20180004164 (accessed on 2025-03-22).

3. Trabert R, Klesh A, Senatore P, Martinchek P, Becker D, Chou A, *et al*. The eXtendable Solar Array System: A Modular Nanosatellite Power System. AIAA-2010-7654. AIAA/AAS Astrodynamics Specialist Conference; 2010 Aug 2–5; Toronto, Ontario, Canada. Available from: https://hdl.handle.net/2027.42/83636 (accessed on 2025-03-22).
4. Patmont CS, Balestrino S, *et al*. Design and Characterization of a Spring Steel Hinge for Deployable CubeSat Structures. Journal of Small Satellites. 2016;5(1):407–418. Available from: https://www.jossonline.com/storage/2021/08/Final-Patmont-Design-and-Characterization-of-a-Spring-Steel-Hinge-for-Deployable-CubeSat-Structures.pdf (accessed on 2025-03-22).
5. PVsyst SA. Cosine Effect. Available from: https://www.pvsyst.com/help/project-design/shadings/backtracking-strategy/cosine-effect.html (accessed on 2025-03-22).
6. California Polytechnic State University. CubeSat Design Specification. Rev. 13. San Luis Obispo (CA): California Polytechnic State University; 2020. Available from: https://www.cubesat.org/resources (accessed on 2025-03-22).
7. GomSpace A/S. Deployable Solar Panel and Hinge Assembly Datasheets. Available from: https://gomspace.com/product/nanopower-dsp/ (accessed on 2025-03-22).
8. Innovative Solutions In Space (ISISpace). CubeSat Deployable Systems Product Catalogue. Available from: https://www.isispace.nl/product/small-satellite-solar-panels/ (accessed on 2025-03-22).
9. National Aeronautics and Space Administration. Shape Distribution of Fragments from Microsatellite Impact Tests. Available from: https://ntrs.nasa.gov/citations/20090007799 (accessed on 2025-03-22).
10. Wijker J. Spacecraft Structures. Berlin: Springer; 2008.